



Motional-state analysis of a trapped ion by ultranarrowband composite pulses










Downloaded from: <https://research.chalmers.se>, 2024-12-23 07:28 UTC

Citation for the original published paper (version of record):

Mallweger, M., Guevara-Bertsch, M., Torosov, B. et al (2024). Motional-state analysis of a trapped ion by ultranarrowband composite pulses. PHYSICAL REVIEW A, 110(5).
<http://dx.doi.org/10.1103/PhysRevA.110.053103>

N.B. When citing this work, cite the original published paper.

Motional-state analysis of a trapped ion by ultranarrowband composite pulses

Marion Mallweger ^{1,*}, Milena Guevara-Bertsch ^{2,3,*}, Boyan T. Torosov ⁴, Robin Thomm ¹, Natalia Kuk ¹, Harry Parke¹, Christan F. Roos ^{2,3}, Gerard Higgins ^{1,5,6}, Markus Hennrich ¹ and Nikolay V. Vitanov ⁷

¹Department of Physics, [Stockholm University](#), SE-106 91 Stockholm, Sweden

²Institut für Experimentalphysik, [Universität Innsbruck](#), Technikerstrasse 25, 6020 Innsbruck, Austria

³Institut für Quantenoptik und Quanteninformation,

Österreichische Akademie der Wissenschaften, Technikerstrasse 21a, 6020-Innsbruck, Austria

⁴Institute of Solid State Physics, [Bulgarian Academy of Sciences](#), 72 Tsarigradsko chaussée, 1784 Sofia, Bulgaria


⁵Department of Microtechnology and Nanoscience (MC2), [Chalmers University of Technology](#), SE-412 96 Gothenburg, Sweden

⁶Institut für Quantenoptik und Quanteninformation (IQOQI),

Österreichische Akademie der Wissenschaften, Boltzmannngasse 3, A-1090 Vienna, Austria

⁷Center for Quantum Technologies, Department of Physics,

[St Kliment Ohridski University of Sofia](#), 5 James Bourchier blvd, 1164 Sofia, Bulgaria

 (Received 10 March 2024; revised 22 August 2024; accepted 16 October 2024; published 7 November 2024)

In this work, we present a method for measuring the motional state of a two-level system coupled to a harmonic oscillator. Our technique uses ultranarrowband composite pulses on the blue sideband transition to scan through the populations of the different motional states. Our approach does not assume any previous knowledge of the motional state distribution and is easily implemented. It is applicable both inside and outside of the Lamb-Dicke regime. For higher phonon numbers especially, the composite pulse sequence can be used as a filter for measuring phonon number ranges. We demonstrate this measurement technique using a single trapped ion and show good detection results with the numerically evaluated pulse sequence.

DOI: [10.1103/PhysRevA.110.053103](https://doi.org/10.1103/PhysRevA.110.053103)

The motional state of a trapped ion plays an essential role in most experiments: Not only is it used for quantum information processing [1], it also has to be very accurately determined for quantum metrology measurements, as it can cause frequency shifts [2–4]. Due to the importance of motion in trapped ion experiments, various schemes have been developed for motional state detection of the mean phonon number or even the phonon number distribution [5–13]. However, most detection methods assume prior knowledge about the initial phonon distribution. Alternatively, one can utilize electron shelving and quantum state engineering techniques to fully determine the quantum state of the ion [14]. For the majority of detection schemes, which rely on coupling individual phonon number changing transitions, extending the technique to higher phonon numbers can be difficult, as changes in the phonon number-dependent coupling strength become harder to distinguish.

Composite pulses allow for the creation of a narrow excitation profile where the coupling to phonon-number changing transitions only occurs in a narrow band of motional energies [15]. This method was originally developed for the study of nuclear magnetic resonances [16]. It can be implemented to measure the motional state of the ion and can be easily extended to higher phonon numbers since it facilitates the filtering of any detection event outside of a chosen fixed band of motional energies. Composite pulses have been successfully implemented in quantum optics [17,18] and quantum information [19–21].

In this work, we present how the motional state of a laser-cooled ion can be measured independently of the distribution of the motional quanta, using a composite pulse sequence. We not only test the composite pulse method for low phonon numbers, but also investigate a regime with hundreds of phonons. Our method can, in principle, be applied both in and outside the Lamb-Dicke regime, assuming the blue-sideband (BSB) Rabi frequencies are well separated. To get a full characterization of the motional state of the ion we propose a sequence of single-shot measurements where different phonon numbers are probed. This technique offers the advantage of providing a characterization of the motional state population within one experimental run, without the need to reinitialize the state.

The measurements were performed on two different experimental setups both using a single ion trapped in a linear Paul trap, one using a $^{88}\text{Sr}^+$ ion and the other a $^{40}\text{Ca}^+$ ion (see Appendices A and B). The method is not restricted to trapped ion experiments, but works analogously in any other

*These two authors contributed equally to this work.

[†]Contact author: marion.mallweger@fysik.su.se

[‡]Contact author: milena.guevara-bertsch@uibk.ac.at

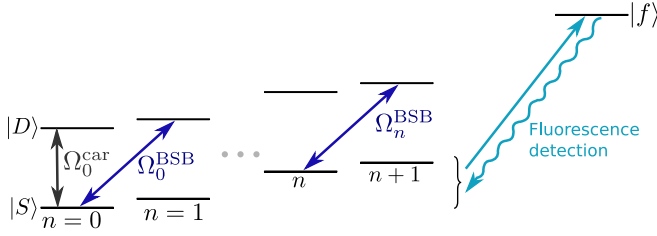


FIG. 1. The level scheme used for our measurements consists of two electronic states, with the ground state $|S\rangle$ and the metastable excited state $|D\rangle$, coupled to motional states with phonon number n . The coupling strength Ω_0^{car} of the carrier transition does not depend strongly on the phonon number, whereas the coupling strength of the blue sideband transition (BSB), Ω_n^{BSB} , scales dependent on n . For measurements of the electronic state, fluorescence detection via a short-lived third level is being used.

two-level system coupled to a harmonic oscillator where the phonon number solely affects the coupling strength, but not the coupling frequency of the transition. The combination of a two-level system, composed of a ground state $|S\rangle$ and an excited state $|D\rangle$, with a quantum harmonic oscillator generates a ladderlike structure, as illustrated in Fig. 1. Blue- and red-sideband transitions (BSB and RSB), detuned from the two-level system by the harmonic oscillator frequency can be used to add or remove a phonon between different levels making it possible to move up or down the ladder structure in a controlled way. For the case of trapped ions, the two-level system is realized by two (meta-)stable states and the harmonic oscillator is given by one of the motional modes. The BSB coupling strength is given by

$$\Omega_n^{\text{BSB}} = \Omega_0^{\text{car}} e^{-\frac{\eta^2}{2}} \eta \sqrt{\frac{1}{n+1}} L_n^1(\eta^2) \approx \eta \Omega_0^{\text{car}} \sqrt{n+1}, \quad (1)$$

where Ω_0^{car} denotes the coupling strength of the ground state transition $|S, 0\rangle \leftrightarrow |D, 0\rangle$, η is the Lamb-Dicke parameter and L_n^1 labels the Laguerre polynomial. Within the Lamb-Dicke regime, meaning for lower phonon numbers, the approximation becomes valid.

Depending on the Lamb-Dicke parameter, the phonon number and the initial coupling strength, Ω_n^{BSB} can vary significantly between adjacent BSB transitions. For lower n , the increase of the coupling strength is usually more significant than for high phonon numbers. This can be seen at the slope of the coupling strength of the BSB in Fig. 2(a). The steeper the slope, the easier it is to resolve a specific BSB transition. However, the opposite is also true; for cases where the slope is less pronounced, a single π -pulse on the BSB transition also excites neighboring BSB transitions. The implementation of composite pulses offers a solution to this problem up to $\eta \lesssim 0.3$, where the BSB transitions get too close such that even UN cannot resolve the transition individually anymore.

The main idea of the ultranarrowband (UN) composite pulse method is to use a sequence of pulses to perform an effective π pulse on a single BSB transition [15]. Each pulse has a different relative phase, generating an effective π pulse only for one specific coupling strength while minimizing the

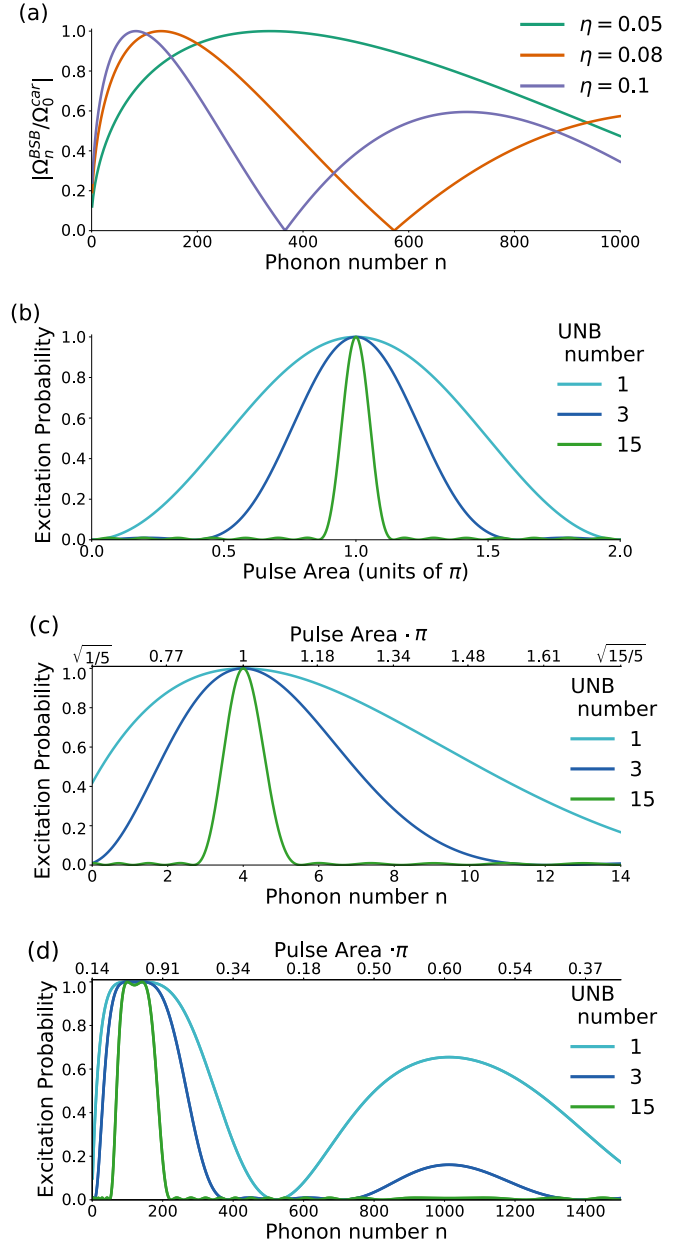


FIG. 2. Composite pulses allow for thermometry on trapped ions. (a) The coupling strength of the BSB transition is dependent on the phonon number and the Lamb-Dicke parameter η . (b) The pulse area gets narrower with an increasing number of composite pulses with optimized phases. (c) Composite pulse sequence applied to detection of a four-phonon Fock state. (d) An increasing number of composite pulses also shows an selective excitation profile for $n = 100$ phonons.

excitation of other neighboring phonon number changing transitions. By increasing the number of UN pulses, the excitation profile can be squeezed as much as desired. This, however, comes at the cost of a longer pulse sequence which may suffer a reduced effectiveness depending on the coherence time of the experimental system. The UN excitation profiles for different numbers of pulses is shown in Fig. 2, and the individual phase values can be found in the Appendix C. Figures 2(b) and 2(c) show an explicit simulated example

of the excitation profile for different UN sets: For Fig. 2(c), the ion is assumed to be initialized in state $|S, 4\rangle$ before applying the composite pulse sequence for detection of $n = 4$. The lower horizontal axis shows the phonon number n , the horizontal axis at the top gives the values of the pulse area in units of π . A pulse area of π hence represents a total flip from $|S, n\rangle$ to $|D, n + 1\rangle$. In Fig. 2(d) for higher phonon numbers ($n = 100$) the excitation probability as a function of the phonon number is presented for different probing schemes. The figure shows how the excitation profile is narrowed with the implementation of more composite pulses in the sequence, thus producing a more precise filter for motional states outside of the specified range.

We demonstrate the effectiveness of the technique for lower phonon number measurements, in the range of $0 \leq n < 10$ using UN composite pulse sequences with a single $^{88}\text{Sr}^+$ ion in a linear Paul trap [4]. In this experimental system, we use the $|S\rangle \equiv |5^2S_{1/2}, m_J = -\frac{1}{2}\rangle \leftrightarrow |D\rangle \equiv |4^2D_{5/2}, m_J = -\frac{5}{2}\rangle$ transition as electronic two-level system. The state readout of the two electronic levels is done via state-dependent fluorescence detection using the $5^2S_{1/2} \leftrightarrow 5^2P_{1/2}$ transition. The motional degrees of freedom of the ion in the trap behave like a linear quantum harmonic oscillator. We couple the internal electronic states of the ion with the motional modes by using external laser fields. This results in BSB with the same resonance frequency but different Rabi frequencies, as needed for the UN pulses. The phonon state preparation and UN composite pulse detection sequence is performed on one of the radial modes.

Before detection of the phonon number n , we first cool the trapped $^{88}\text{Sr}^+$ ion close to its motional ground state using Doppler and sideband cooling, initializing the ion in $|S, 0\rangle$. To add a motional quantum, we drive a π -pulse on the BSB transition from $|S, 0\rangle$ to the excited state $|D, 1\rangle$, followed by a π pulse on the carrier transition, as described in Ref. [6]. This brings the ion to the state $|S, 1\rangle$. Repeating the sequences m times will result in a phonon number increase of m . For the detection of n , BSB pulses given by the UN pulse sequence are applied. For the detection of n , BSB pulses given by the UN pulse sequence are applied. During the fluorescence detection there are then two possible outcomes: If the prepared phonon number does not match the probed one, the ion will end up in the $|S\rangle$ state and scatter photons during the fluorescence detection, changing the motional state. If the prepared phonon number matches the probed one, the ion will end up in the $|D\rangle$ state, and no photons will be scattered. Note that after this step, the phonon number will be increased by one motional quanta.

For the low phonon number regime we prepared Fock states $|m\rangle$ from $m = 0$ to $m = 9$ and probed Fock states $|n\rangle$ from $n = 0$ to $n = 9$ using the UN pulse sequence. The absence of fluorescence indicates $n = m$ leaving the ion in the state $|D, n + 1\rangle$. After the state detection was performed the ion was again cooled and initialized in the desired state.

The measurements were done for multiple UN pulse sequences consisting of increasing pulse numbers. The results are shown in Fig. 3. Increasing the number of pulses increases the precision of the detection. The experimental data is in good agreement with the theoretical prediction, described in

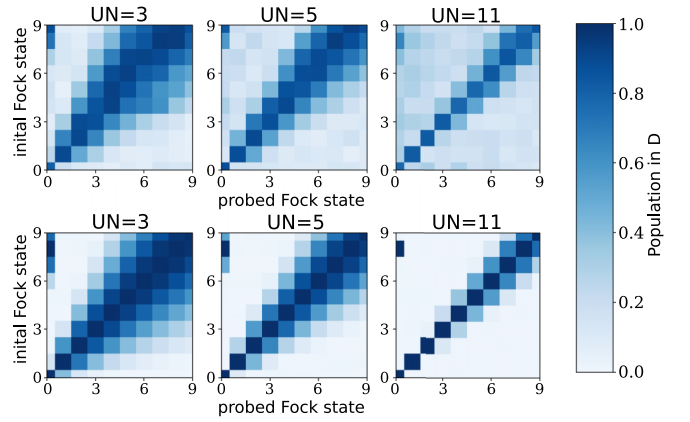


FIG. 3. Motional state detection using composite pulses. The top row shows our experimental results, and the bottom row shows the theoretical simulations. Using BSB pulses the ion was initialized in different Fock states (vertical axis) and afterwards the different motional states were probed using UN pulses (horizontal axis). The off diagonal excitation decreases with a higher number of UN pulses, leading to more precise results of motional state detection. The experimental data in the top row shows some minor off-diagonal excitation due to excitation of other adjacent transitions and imperfect phonon number state preparation. The maximum excitation of the experimental data is limited coherence time of the carrier and foremost the BSB transition. The results were obtained with 100 cycles per data point.

the Appendix C. The increased background of the experimental data can be explained by phase and intensity fluctuations of the laser and excitation due to other adjacent transitions. The maximum excitation of the experimental data is limited by the coherence time of the carrier and the BSB transition, caused by dephasing and motional heating. Imperfect Fock state preparation will lead to off-diagonal excitations in Fig. 3. The composite pulse scheme shows a high detection efficiency for $n = m$. Using the technique described above followed by a π pulse on the RSB transition, it is possible to efficiently verify and continue using the desired motional state in subsequent measurements. For the case $n \neq m$ a higher number of pulses leads to a narrower excitation profile and therefore less excitation of neighboring BSB transitions, which can be clearly seen. Especially for UN=11 excitations for $n \neq m$ remain negligible for low n . When working with lower lying phonon number states as shows in Fig. 3, an excitation signal reoccurs at $n = 7$ because the transition $|g, 8\rangle \rightarrow |e, 9\rangle$ has a relative coupling strength $\sqrt{8+1} = 3$. Hence a π pulse on the first transition will be seen as a 3π pulse on this transition, which too causes complete population transfer, due to the periodicity of the UN pulses.

These methods can be used to measure the motional state in the Fock basis in a single experiment run, similar as shown in [22]. This involves conducting a series of yes/no tests, successively testing whether or not $n = 0$, $n = 1$, $n = 2$, etc. These tests should be set up such that the ion only scatters light if the probed phonon number matches the motional state of the ion. In this case the measurements are nondisruptive until the correct phonon number is probed. The fraction of cycles during which light is scattered will not be counted for the

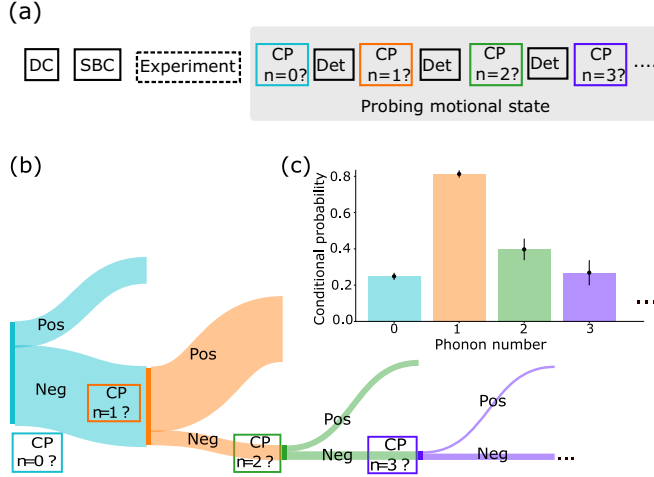


FIG. 4. Single-shot measurement using a set of five composite pulses. (a) The probing scheme starts by Doppler cooling and sideband cooling (DC and SBC), followed by a chosen experiment. To probe the motional state of the ion a series of composite pulses (CP) and detection (Det) pulses are performed probing different phonon numbers (n). If the result of a probing pair for a given phonon number is positive (Pos) the measurement stops, if it is negative (Neg) the next phonon number is probed. (b) A Sankey diagram shows an example of the outcome of a measurement set where the ion was prepared with a phonon number equal to 1. As expected, the majority of positive events come after the probing pair for $n=1$. Positive events from the other probing pairs can be explained by noise and excitation due to other adjacent transitions. (c) The bar diagram gives a conditional probability for the test of this phonon number given that all previous phonon numbers were tested negative. The data presented uses a total of 483 cycles. Error bars represent quantum projection noise (68% confidence intervals).

following phonon number measurements, hence the number of cycles reduces for increasing number of probed phonons. A sequence involving successive tests from $\langle n \rangle = 0$ to $\langle n \rangle = 3$ is presented in Fig. 4(a). This was experimentally implemented, and used to probe a trapped ion which was (nominally) prepared in the $n = 1$ state, the results are shown in Figs. 4(b) and 4(c). Experimental imperfections cause the false positives (positive outcomes to the $\langle n \rangle = 0$, $\langle n \rangle = 2$, $\langle n \rangle = 3$ tests) and the false negatives (negative outcomes to the $\langle n \rangle = 1$ test). This method increases the amount of information about the motional state that can be gained from a single experiment run, which may be particularly useful in experiments with relatively low repetition rates, such as atom-ion collision experiments [23–25]. The method can be also implemented as an alternative way to characterize nonthermal motional state distribution after laser cooling necessary for the estimation of secular motion time-dilation shifts in optical clocks [2,26,27].

To demonstrate the application of the UN composite pulses technique in the regime of hundreds of phonons, a single $^{40}\text{Ca}^+$ ion in a linear Paul trap [28] was used. In this experimental system we use the $|S\rangle \equiv |4^2S_{1/2}, m_J = \frac{1}{2}\rangle \leftrightarrow |D\rangle \equiv |3^2D_{5/2}, m_J = \frac{3}{2}\rangle$ transition as electronic two-level system. The detection of the ion is done via state-dependent fluorescence detection using the $4^2S_{1/2} \leftrightarrow 4^2P_{1/2}$ transition. As for the case of the strontium ion, the motional degrees of freedom

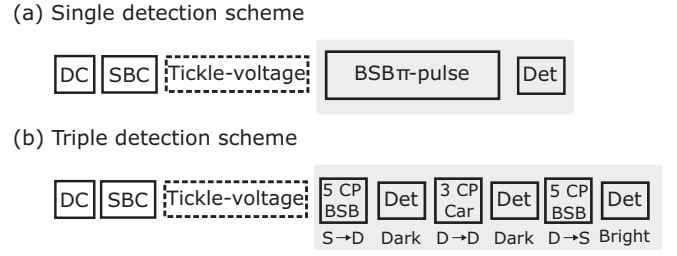


FIG. 5. Detection schemes for high phonon numbers. Both schemes start by Doppler cooling and sideband cooling the ion (DC and SBC) followed by the application of a weak electric field pulse with tunable frequency and intensity (tickle-voltage). (a) The single detection is followed by a BSB π pulse and a detection pulse. This scheme is used to calibrate the tickle voltage. The frequency, pulse length, and intensity are calibrated by comparing the obtained excitation profile with the expected theoretical profile as illustrated in Fig. 2. (b) The triple detection scheme consist of three sets of composite pulses followed each by a detection pulse: five composite pulses on the BSB, three composite pulses on the carrier and five composite pulses on the BSB transition. If the motional state of the ion is on the desired phonon range the population is transferred in the first set from the S to the D state, from D to D in the second and from D back to S in the third set. The ion is considered to be in the desired phonon range if the results of the detection pulses are “Dark”, “Dark” and “Bright”.

of the calcium ion in the trap behave like a quantum harmonic oscillator, allowing the coupling of the internal electronic states of the ion with the motional modes using external laser fields. For this measurement set the phonon adding and UN composite pulse sequences are performed on the axial mode.

We start by cooling the trapped $^{40}\text{Ca}^+$ ion close to its motional ground state using Doppler and sideband cooling, initializing the ion in the $|S, 0\rangle$ ground state. To add the desired motional quanta, a weak electric field with a tunable frequency, referred to as the “tickle voltage” in the rest of the text, is applied by means of an electrode situated at the bottom of the trap to excite the axial motional mode of the ion. By controlling the pulse duration and intensity of the tickle voltage and using a frequency slightly detuned (≈ 600 Hz) from the resonance with the motional mode, the ion can be coherently excited. To calibrate the tickle voltage, we apply the single detection scheme, described in Fig. 5(a) where a single BSB π and a detection pulse are applied after the tickle-voltage pulse. The pulse length is scanned and thus the phonon number is varied, following the excitation profile described in Fig. 2. In this case, since only a single pulse is applied the excitation profile exhibits several maxima. To access different motional energy ranges the axial confinement of the trap is modified by changing the voltage of the end-cap electrodes.

For the detection of the phonon number in the desired range we implemented a triple detection scheme: Three sets of UN composite pulses followed by a detection pulse are applied. The first set is composed by five composite pulses on the BSB, if the motional energy of the ion is in the desired phonon range, this pulse sequence transfers the population from $|S\rangle$ to $|D\rangle$ and a “dark” event is detected during the fluorescence excitation. The second set is composed by three composite carrier pulses, used to depump events with lower

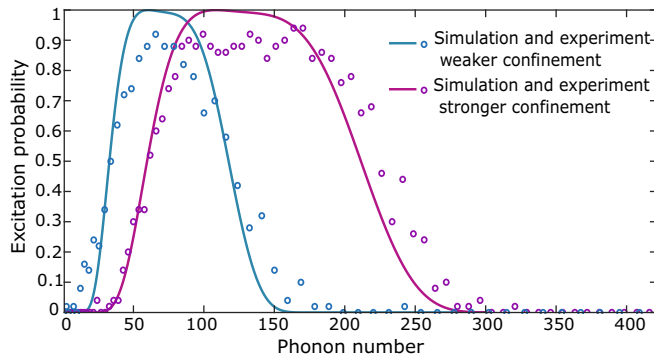


FIG. 6. By scanning the pulse length of the “tickle voltage” using a slightly detuned frequency (≈ 600 Hz) the mean phonon number is “scanned”. The excitation probability using the triple detection scheme is measured as a function of the mean phonon number. The measured data for two different axial confinements (blue circles for 742 kHz and purple for 1.329 MHz) matches closely the predicted theoretical calculations (blue and pink solid lines).

phonon numbers outside of the desired range, due to heating rate for example. An event where the ion is in the desired phonon range would not be affected by this set of composite pulses, the ion will remain in the D state and detected as “dark”. On the contrary a “bright” event would reveal that the ion was outside of the desired phonon range. Finally a third set of composite pulses on the BSB is applied to transfer the population back to the S state. When the energy of the ion is in the selected range the result of the measurement is: “dark”, “dark”, and “bright”. The implementation of this triple detection scheme ensures a suppression of any excitation probability outside of the desired range to about 10^{-4} . For reference, if only one set of UN composite pulses is implemented on the BSB the excitation probability outside of the desired range is suppressed to about 10^{-2} .

As illustrated in Fig. 6 the technique is successfully implemented to detect two distinct energy ranges, using an axial frequency of 742 kHz and 1.329 MHz. The measured excitation probability as a function of the mean phonon number for both energy ranges is in close agreement with the theoretical estimations described and illustrated at the beginning of the paper in Fig. 2. As can be seen in the figure, only energies in the defined energy ranges are detected as “positive” events by the triple detection method: between 35 and 119 phonons for the weak trap setting with 742 kHz axial confinement and between 63 and 213 phonons for the strong trap at 1.329 MHz. As can be seen in Fig. 6, the excitation of the measured data points does not reach the maximum value, this effect can be explained on one side by decoherence processes (electric or magnetic field noise) during the 13 pulses, or it can also be explained by imperfections on the coherent excitation of the ion by means of the “tickle voltage”.

The single-phonon measurement technique can be implemented in a nondemolition fashion. Nondemolition measurements [29] are special measurement operations, they project the system onto eigenvectors of the measurement operator. Repeating a nondemolition measurement results in the same outcome. To implement a non-demolition, we must contend with the disruption caused by the scattering of fluorescence

light. In a measurement that probes whether the phonon number is n , with fluorescence indicating a positive result, if fluorescence is detected the measurement operation should be expanded to include ground state cooling followed by excitation of the n -phonon Fock state [30]. Then, if there is a positive outcome indicating that the phonon state had been n , the scattering of fluorescence light disrupts the state, but then the disruption is undone and the n -phonon state is prepared. If there is a negative outcome, on the other hand, the phonon state is not disrupted by fluorescence scattering.

In this work we have presented a method for measuring the motional state of a trapped ion using suitable, ultra-narrowband, composite pulses. Our approach is based on a systematic scan of the populations of the phonon state or range. Our method can be seen as an alternative to other traditional methods. It works for $\eta \lesssim 0.3$ and hundreds of phonons. The technique has the advantage that it can facilitate the design of single-shot measurement schemes to probe the motional state of the ion after any given operation. We have presented the implementation of a scheme that probes in a single run the occupation of different phonon numbers. The measurements performed with single trapped ions of different species show good agreement with the numerical prediction using UN pulses, in the regime of low as well as high phonon numbers. An increase in pulse number also results in a higher accuracy of determining the motional state but comes at a cost of a longer pulse sequences which might exceed the coherence time.

While other techniques will give a more accurate result of the phonon state, especially in the lower phonon number regime, the composite pulse method can be easily implemented in any two-level system coupled to the harmonic oscillator of interest. This might be particularly useful if one needs a lightweight and easy to implement method to test if a single Fock state is populated. For higher phonon numbers it can be used as a filter to determine if the phonon number is in the desired range or not.

The experimental work was also supported by the Knut & Alice Wallenberg Foundation through the Wallenberg Centre for Quantum Technology [WACQT], by the Swedish Research Council (Grants. No. 2017-04638, No. 2020-00381, and No. 2021-05811), by the Carl Trygger Foundation, by the Olle Engkvist Foundation, and by the Bulgarian national plan for recovery and resilience, Contract No. BG-RRP-2.004-0008-C01 (SUMMIT), Project No. 3.1.4 (AQOT). This project has also received funding from the European Unions Horizon Europe research and innovation program under Grant Agreement No. 101046968 (BRISQ). We also acknowledge funding from the Institut für Quanteninformation GmbH.

APPENDIX A: EXPERIMENTAL SETUP—STOCKHOLM UNIVERSITY

The measurements for detection of lower phonon numbers were performed with a single trapped $^{88}\text{Sr}^+$ in a linear Paul trap. For each individual experimental run, Doppler cooling was performed on the $5^2S_{1/2} \leftrightarrow 5^2P_{1/2}$ transition, afterwards the motional ground state was reached by sideband cooling on

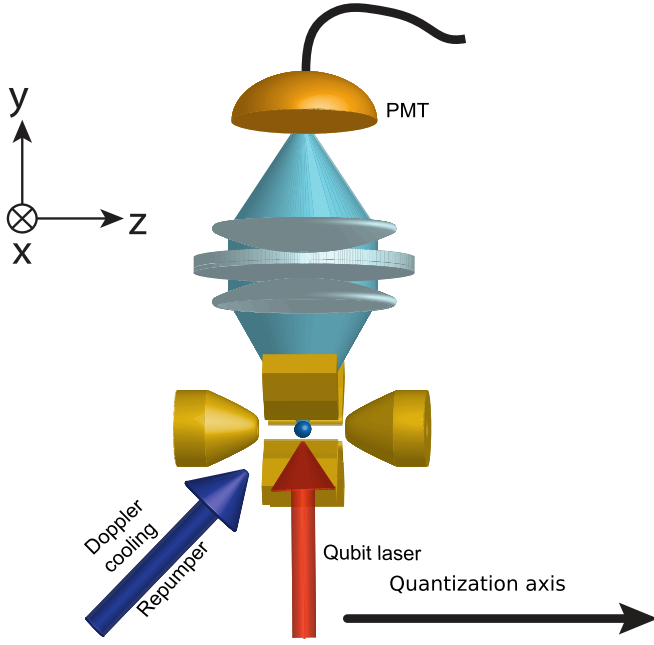


FIG. 7. The ion is trapped using a linear Paul trap. The cooling and repump lasers are applied 45° to the trap axis, the qubit laser is applied radially (on the horizontal plane) with 90° to the trap axis. Fluorescence is detected by collecting light with a large numerical aperture lens and directing it onto a photomultiplier tube (PMT) mounted at the top of the experiment.

the radial modes. After the cooling steps, the ion was optically pumped into the state $|S\rangle \equiv 5^2S_{1/2}, m_J = -\frac{1}{2}$.

All operations on the electronic two-level transition $|S\rangle \leftrightarrow |D\rangle$, with $|D\rangle \equiv 4^2D_{5/2}, m_J = -\frac{5}{2}$, were performed with a single beam that is perpendicular to the trap axis and which had a 45° overlap with each of the two radial modes. Fluorescence detection was performed using a photomultiplier tube (PMT) mounted at the top of the chamber, by excitation of the $5^2S_{1/2} \leftrightarrow 5^2P_{1/2}$ transition. During Doppler cooling and detection sequences a repumping laser at 1092 nm, driving the transition $4^2D_{3/2} \leftrightarrow 5^2P_{1/2}$, was also used to remove any population that spontaneously decays into the metastable $4^2D_{3/2}$ state. A sketch of the setup is shown in Fig. 7.

The composite pulse sequences were performed on a blue sideband (BSB) transition on a radial mode of the ion with the Lamb-Dicke parameter $\eta = 0.036$. The radial sideband was detuned from the carrier transition by $\Delta = 2\pi \times 1.74$ MHz and the coupling strength for the transition $|S, n=0\rangle \leftrightarrow |D, n=1\rangle$ was $\Omega_0 = 2\pi \times 5.04(3)$ kHz. The measured heating rate of the radial mode used for the experimental sequence was 13.7(4) quanta/s.

APPENDIX B: EXPERIMENTAL SETUP—UNIVERSITY OF INNSBRUCK

The measurements for the higher phonon numbers were performed with a single trapped $^{40}\text{Ca}^+$ in a linear Paul trap. The transition $4^2S_{1/2} \leftrightarrow 4^2P_{1/2}$ at 397 nm is used for Doppler cooling and internal state discrimination in combination with the $3^2D_{3/2} \leftrightarrow 4^2P_{1/2}$ transition at 866 nm, the $3^2D_{5/2} \leftrightarrow 4^2P_{3/2}$ at 854 nm is used as a repumper for efficient state

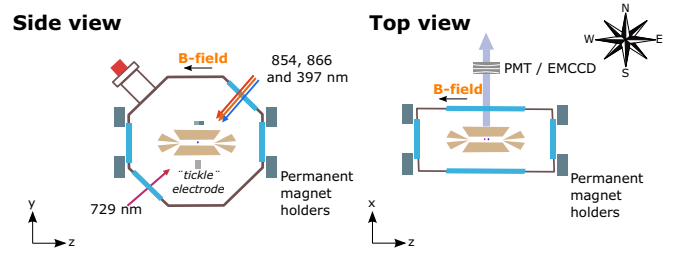


FIG. 8. A $^{40}\text{Ca}^+$ ion is trapped using a linear Paul trap. The different lasers and imaging directions are illustrated with respect to the cardinal directions (indicated by the compass rose). The magnetic quantization field (B field) along the z-axis of the trap is provided by a pair of concentric permanent magnet holder situated in the west and east viewports of the chamber. The “tickle” voltage electrode is situated below the trap along the y axis. The fluorescence emitted by the ion is detected by a photomultiplier tube and an electron multiplying charge-coupled device camera through the northern viewport.

preparation. The $4^2S_{1/2} \leftrightarrow 3^2D_{5/2}$ quadrupole transition at 729 nm is used for two-level operations using a single beam orthogonal to the quantization axis. The same transition in combination with the 854 nm is used for sideband cooling. The fluorescence is split and detected using both a PMT and an electron multiplying charge-coupled device camera through the northern viewport as shown in Fig. 8.

To add the desired motional quanta to the axial motional mode of the single ion, a weak electric field with a tunable frequency is applied by means of a “tickle” electrode situated at the bottom of the trap.

APPENDIX C: ULTRANARROWBAND COMPOSITE PULSE SEQUENCE

Table I lists UN composite pulse sequences, which was used for the presented measurements. A measure of the performance of these sequences is the dimensionless parameter α , which measures the width of the excitation profile, outside of which the excitation probability is ≤ 0.01 . For a single resonant pulse the value of α is 0.936.

TABLE I. UN composite sequences which produce significant excitation inside the range $[\pi(1-\alpha), \pi(1+\alpha)]$, and negligible excitation below 0.01% outside this range.

CP	Phases ($\phi_1, \phi_2, \dots, \phi_N$)	α
UN3	(0, 0.587, 1.174) π	0.551
UN5	(0, 0.237, 1.583, 0.929, 1.166) π	0.361
UN7	(0, 0.299, 0.972, 0.850, 0.727, 1.400, 1.700) π	0.265
UN9	(0, 0.392, 0.032, 1.996, 0.597, 1.199, 1.164, 0.805, 1.198) π	0.209
UN11	(0, 0.429, 0.380, 0.931, 1.285, 0.991, 0.695, 1.047, 1.598, 1.551, 1.982) π	0.172
UN13	(0, 0.182, 1.949, 1.435, 1.008, 1.424, 1.256, 1.084, 1.491, 1.057, 0.544, 0.321, 0.514) π	0.146
UN15	(0, 0.021, 0.512, 0.894, 0.841, 0.475, 0.940, 1.059, 1.166, 1.625, 1.264, 1.212, 1.604, 0.095, 0.101) π	0.127

For the first two transitions $|0\rangle \rightarrow |1\rangle$ and $|1\rangle \rightarrow |2\rangle$ to be separated (with a contribution of less than 1% from the other transition), we must have $\alpha < \sqrt{2} - 1 \approx 0.414$. As Table I shows, ultranarrowband (ultra-NB) sequences of five or more pulses can achieve this separation, meaning that the signal for the first peak $|0\rangle \rightarrow |1\rangle$ will be accurate up to 1% error (the second peak has also a contribution from the third transition $|2\rangle \rightarrow |3\rangle$). If we wish to separate the first three transi-

tions $|0\rangle \rightarrow |1\rangle$, $|1\rangle \rightarrow |2\rangle$ and $|2\rangle \rightarrow |3\rangle$, we must have $\alpha < \sqrt{3/2} - 1 \approx 0.225$. As Table I shows, ultra-NB sequences of nine or more pulses can achieve this separation. In this case the signals from the first two peaks $|0\rangle \rightarrow |1\rangle$ and $|1\rangle \rightarrow |2\rangle$ will be accurate up to 1% error. Finally, if we wish to separate the first four transitions, from $|0\rangle \rightarrow |1\rangle$ to $|3\rangle \rightarrow |4\rangle$, we must have $\alpha < \sqrt{4/3} - 1 \approx 0.155$. As Table I shows, ultra-NB sequences of 13 or more pulses can achieve this separation.

-
- [1] D. Leibfried, R. Blatt, C. Monroe, and D. Wineland, Quantum dynamics of single trapped ions, *Rev. Mod. Phys.* **75**, 281 (2003).
 - [2] C. W. Chou, D. B. Hume, J. C. J. Koelemeij, D. J. Wineland, and T. Rosenband, Frequency comparison of two high-accuracy Al^+ optical clocks, *Phys. Rev. Lett.* **104**, 070802 (2010).
 - [3] T. Rosenband, D. B. Hume, P. O. Schmidt, C. W. Chou, A. Brusch, L. Lorini, W. H. Oskay, R. E. Drullinger, T. M. Fortier, J. E. Stalnaker, S. A. Diddams, W. C. Swann, N. R. Newbury, W. M. Itano, D. J. Wineland, and J. C. Bergquist, Frequency ratio of Al^+ and Hg^+ single-ion optical clocks; metrology at the 17th decimal place, *Science* **319**, 1808 (2008).
 - [4] G. Higgins, F. Pokorny, C. Zhang, and M. Hennrich, Highly polarizable Rydberg ion in a Paul trap, *Phys. Rev. Lett.* **123**, 153602 (2019).
 - [5] D. J. Wineland, W. M. Itano, J. C. Bergquist, and R. G. Hulet, Laser-cooling limits and single-ion spectroscopy, *Phys. Rev. A* **36**, 2220 (1987).
 - [6] D. M. Meekhof, C. Monroe, B. E. King, W. M. Itano, and D. J. Wineland, Generation of nonclassical motional states of a trapped atom, *Phys. Rev. Lett.* **76**, 1796 (1996).
 - [7] C. Shen, Z. Zhang, and L.-M. Duan, Scalable implementation of boson sampling with trapped ions, *Phys. Rev. Lett.* **112**, 050504 (2014).
 - [8] S. An, J.-N. Zhang, M. Um, D. Lv, Y. Lu, J. Zhang, Z.-Q. Yin, H. T. Quan, and K. Kim, Experimental test of the quantum Jarzynski equality with a trapped-ion system, *Nat. Phys.* **11**, 193 (2015).
 - [9] M. Um, J. Zhang, D. Lv, Y. Lu, S. An, J.-N. Zhang, H. Nha, M. S. Kim, and K. Kim, Phonon arithmetic in a trapped ion system, *Nat. Commun.* **7**, 11410 (2016).
 - [10] S. Ding, G. Maslennikov, R. Häblützel, and D. Matsukevich, Cross-Kerr nonlinearity for phonon counting, *Phys. Rev. Lett.* **119**, 193602 (2017).
 - [11] R. Ohira, T. Mukaiyama, and K. Toyoda, Phonon-number-resolving detection of multiple local phonon modes in trapped ions, *Phys. Rev. A* **100**, 060301(R) (2019).
 - [12] Z. Meir, T. Sikorsky, N. Akerman, R. Ben-shlomi, M. Pinkas, and R. Ozeri, Single-shot energy measurement of a single atom and the direct reconstruction of its energy distribution, *Phys. Rev. A* **96**, 020701(R) (2017).
 - [13] M. Mallweger, M. H. de Oliveira, R. Thomm, H. Parke, N. Kuk, G. Higgins, R. Bachelard, C. J. Villas-Boas, and M. Hennrich, Single-shot measurements of phonon number states using the Autler-Townes effect, *Phys. Rev. Lett.* **131**, 223603 (2023).
 - [14] D. Leibfried, D. M. Meekhof, C. Monroe, B. E. King, W. M. Itano, and D. J. Wineland, Experimental preparation and measurement of quantum states of motion of a trapped atom, *J. Mod. Opt.* **44**, 2485 (1997).
 - [15] B. T. Torosov, E. S. Kyoseva, and N. V. Vitanov, Composite pulses for ultrabroad-band and ultranarrow-band excitation, *Phys. Rev. A* **92**, 033406 (2015).
 - [16] M. H. Levitt, Composite pulses, *Prog. Nucl. Magn. Reson. Spectrosc.* **18**, 61 (1986).
 - [17] D. Schraft, T. Halfmann, G. T. Genov, and N. V. Vitanov, Experimental demonstration of composite adiabatic passage, *Phys. Rev. A* **88**, 063406 (2013).
 - [18] G. T. Genov, D. Schraft, T. Halfmann, and N. V. Vitanov, Correction of arbitrary field errors in population inversion of quantum systems by universal composite pulses, *Phys. Rev. Lett.* **113**, 043001 (2014).
 - [19] C. Piltz, B. Scharfenberger, A. Khromova, A. F. Varón, and C. Wunderlich, Protecting conditional quantum gates by robust dynamical decoupling, *Phys. Rev. Lett.* **110**, 200501 (2013).
 - [20] F. Schmidt-Kaler, H. Häffner, M. Riebe, S. Gulde, G. P. T. Lancaster, T. Deuschle, C. Becher, C. F. Roos, J. Eschner, and R. Blatt, Realization of the Cirac-Zoller controlled-NOT quantum gate, *Nature (London)* **422**, 408 (2003).
 - [21] U. Poschinger, A. Walther, M. Hettrich, F. Ziesel, and F. Schmidt-Kaler, Interaction of a laser with a qubit in thermal motion and its application to robust and efficient readout, *Appl. Phys. B* **107**, 1159 (2012).
 - [22] Y. Lu, S. An, J.-N. Zhang, and K. Kim, Probing quantum fluctuations of work with a trapped ion, in *Thermodynamics in the Quantum Regime: Fundamental Aspects and New Directions*, edited by F. Binder, L. A. Correa, C. Gogolin, J. Anders, and G. Adesso (Springer International Publishing, New York, 2018), pp. 917–938.
 - [23] E. Trimby, H. Hirzler, H. Fürst, A. Safavi-Naini, R. Gerritsma, and R. Lous, Buffer gas cooling of ions in radio-frequency traps using ultracold atoms, *New J. Phys.* **24**, 035004 (2022).
 - [24] T. Feldker, H. Fürst, H. Hirzler, N. Ewald, M. Mazzanti, D. Wiater, M. Tomza, and R. Gerritsma, Buffer gas cooling of a trapped ion to the quantum regime, *Nat. Phys.* **16**, 413 (2020).
 - [25] A. Mohammadi, A. Krüchow, A. Mahdian, M. Deiß, J. Pérez-Ríos, H. da Silva Jr., M. Raoult, O. Dulieu, and J. H. Denschlag, Life and death of a cold BaRb^+ molecule inside an ultracold cloud of Rb atoms, *Phys. Rev. Res.* **3**, 013196 (2021).

- [26] J.-S. Chen, S. M. Brewer, C. W. Chou, D. J. Wineland, D. R. Leibbrandt, and D. B. Hume, Sympathetic ground state cooling and time-dilation shifts in an $^{27}\text{Al}^+$ optical clock, *Phys. Rev. Lett.* **118**, 053002 (2017).
- [27] N. Huntemann, C. Sanner, B. Lipphardt, C. Tamm, and E. Peik, Single-ion atomic clock with 3×10^{-18} systematic uncertainty, *Phys. Rev. Lett.* **116**, 063001 (2016).
- [28] M. Guggemos, D. Heinrich, O. A. Herrera-Sancho, R. Blatt, and C. F. Roos, Sympathetic cooling and detection of a hot trapped ion by a cold one, *New J. Phys.* **17**, 103001 (2015).
- [29] V. B. Braginsky, Y. I. Vorontsov, and K. S. Thorne, Quantum nondemolition measurements, *Science* **209**, 547 (1980).
- [30] D. Leibfried, D. M. Meekhof, B. E. King, C. Monroe, W. M. Itano, and D. J. Wineland, Experimental determination of the motional quantum state of a trapped atom, *Phys. Rev. Lett.* **77**, 4281 (1996).